Metabolic targeting of hypoxia and HIF1 in solid tumors can enhance cytotoxic chemotherapy

Rob A. Cairns, Ioanna Papandreou, Patrick D. Sutphin, and Nicholas C. Denko*

Division of Radiation and Cancer Biology, Department of Radiation Oncology, Stanford University School of Medicine, Stanford, CA 94305

Edited by Napoleone Ferrara, Genentech, Inc., South San Francisco, CA, and approved April 4, 2007 (received for review December 28, 2006)

Solid tumors frequently contain large regions with low oxygen concentrations (hypoxia). The hypoxic microenvironment induces adaptive changes to tumor cell metabolism, and this alteration can further distort the local microenvironment. The net result of these tumor-specific changes is a microenvironment that inhibits many standard cytotoxic anticancer therapies and predicts for a poor clinical outcome. Pharmacologic targeting of the unique metabolism of solid tumors could alter the tumor microenvironment to provide more favorable conditions for anti-tumor therapy. Here, we describe a strategy in which the mitochondrial metabolism of tumor cells is increased by pharmacologic inhibition of hypoxia-inducible factor 1 (HIF1) or its target gene pyruvate dehydrogenase kinase 1 (PDK1). This acute increase in oxygen consumption leads to a corresponding decrease in tumor oxygenation. Whereas decreased oxygenation could reduce the effectiveness of some traditional therapies, we show that it dramatically increases the effectiveness of a hypoxia-specific cytotoxin. This treatment strategy should provide a high degree of tumor specificity for increasing the effectiveness of hypoxic cytotoxins, as it depends on the activation of HIF1 and the presence of hypoxia, conditions that are present only in the tumor, and not the normal tissue.

hypoxia-inducible factor | HIF inhibitors | pyruvate dehydrogenase kinase | tumor metabolism

Hypoxia is an almost universal feature of solid tumors. Unlike the balance achieved in normal tissues, the consumption of oxygen by tumor tissue is greater than the oxygen delivery from the supplying blood vessels (1, 2). This inadequate and inconsistent perfusion produces extreme spatial and temporal variations in oxygen concentration throughout the tumor mass. Clinically, hypoxia is associated with resistance to standard treatments, especially radiation therapy, and is predictive of metastasis and poor outcome in a variety of tumor types (1, 3–5). Strategies designed to improve tumor oxygenation have been investigated, and, although there is evidence for a small improvement in outcome, no method has been widely accepted into clinical practice (1, 6). An alternative approach to the problem of hypoxia is to exploit this unique situation by developing therapeutic strategies that rely on the presence of hypoxia to achieve tumor specificity (7, 8).

It has long been known that the metabolism of solid tumors is radically different from that in the corresponding normal tissues. Recently, it has become evident that many of the genes involved in malignant transformation, including Myc (9), Akt (10), and p53 (11) have a profound effect on cellular metabolism. In addition to these stable genetic alterations, the hypoxic microenvironment of solid tumors stimulates epigenetic changes in gene expression through the hypoxia-inducible factor 1 (HIF1) transcription factor that also contribute to the metabolic state of tumor cells (12–16). Our increasing understanding of these molecular pathways provides opportunities to specifically target tumor metabolism to overcome physiologic barriers and improve therapy.

Our group (17), along with others (18), recently showed that under hypoxic conditions, HIF1 causes an increase in its target gene pyruvate dehydrogenase kinase 1 (PDK1), which acts to limit the amount of pyruvate entering the citric acid cycle, leading to decreased mitochondrial oxygen consumption. This adaptive response to low oxygen conditions may allow cells to spare molecular oxygen when it becomes scarce, making it available for other critical cellular processes (19). These findings predict that inhibition of HIF1 or PDK1 *in vivo* could alter tumor metabolism and increase oxygen consumption, which would lead to decreased overall tumor oxygenation. Decreased oxygenation in turn would increase the effectiveness of hypoxia targeted therapies such as the hypoxic cytotoxin tirapazamine (TPZ) (7). We tested this hypothesis using echinomycin, a recently identified small molecule inhibitor of HIF1 DNA binding activity (20), and dichloroacetate (DCA), a small molecule inhibitor of PDK1 activity (21).

Results

We first examined the effect of the HIF inhibitor echinomycin on the hypoxic expression of the HIF target gene PDK1 by immunoblot in RKO and Su.86 human tumor cells exposed to hypoxia. The HIF1 targets PDK1, Bnip3, and Bnip3L were induced by hypoxia, and this induction was blocked in the presence of echinomycin (Fig. 1*a*). To establish that this effect was due to HIF1 inhibition, we similarly tested WT and HIF1α knockout mouse embryo fibroblasts (MEFs). Echinomycin treatment blocked PDK1 induction in the WT cells, but had no effect on hypoxic expression of PDK1 in HIF1α deficient cells [supporting information (SI) Fig. 6*a*]. Because PDK1 expression has been shown to inhibit oxygen consumption (17), and echinomycin blocks hypoxic PDK1 expression, we tested echinomycin for its ability to modulate the hypoxic decrease in oxygen consumption. Echinomycin treatment yielded a dose-dependent block to the HIF1-dependent reduction in oxygen consumption in parental RKO cells, but had no effect on the oxygen consumption in RKOShHIF1α cells (Fig. 1 *b* and *c*). Similar effects of echinomycin on oxygen consumption were observed in the Su.86 (Fig. 1*b*) and MEF cell lines (SI Fig. 6*b*). These genetically matched cells show that echinomycin treatment can block the adaptive HIF1 dependent drop in oxygen consumption (Fig. 1 *b* and *c*).

We next examined the effect of genetic and biochemical inhibition of HIF1 on oxygen consumption *in vivo*. Because HIF1 is not required for the growth of colon cancer xenografts (22, 23) (SI Fig. 7), RKO and RKOShHIF1α cells were grown as tumors

Author contributions: R.A.C. and I.P. contributed equally to this work; R.A.C., I.P., and N.C.D. designed research; R.A.C., I.P., P.D.S., and N.C.D. performed research; P.D.S. contributed new reagents/analytic tools; R.A.C., I.P., and N.C.D. analyzed data; and R.A.C. and N.C.D. wrote the paper.

The authors declare no conflict of interest.

This article is a PNAS Direct Submission.

Abbreviations: HIF, hypoxia-inducible factor; PDK1, pyruvate dehydrogenase kinase 1; DCA, dichloroacetate; TPZ, tirapazamine; MEF, mouse embryo fibroblast; PI, propidium iodide.

*To whom correspondence should be addressed. E-mail: ndenko@stanford.edu.

This article contains supporting information online at www.pnas.org/cgi/content/full/0611662104/DC1.

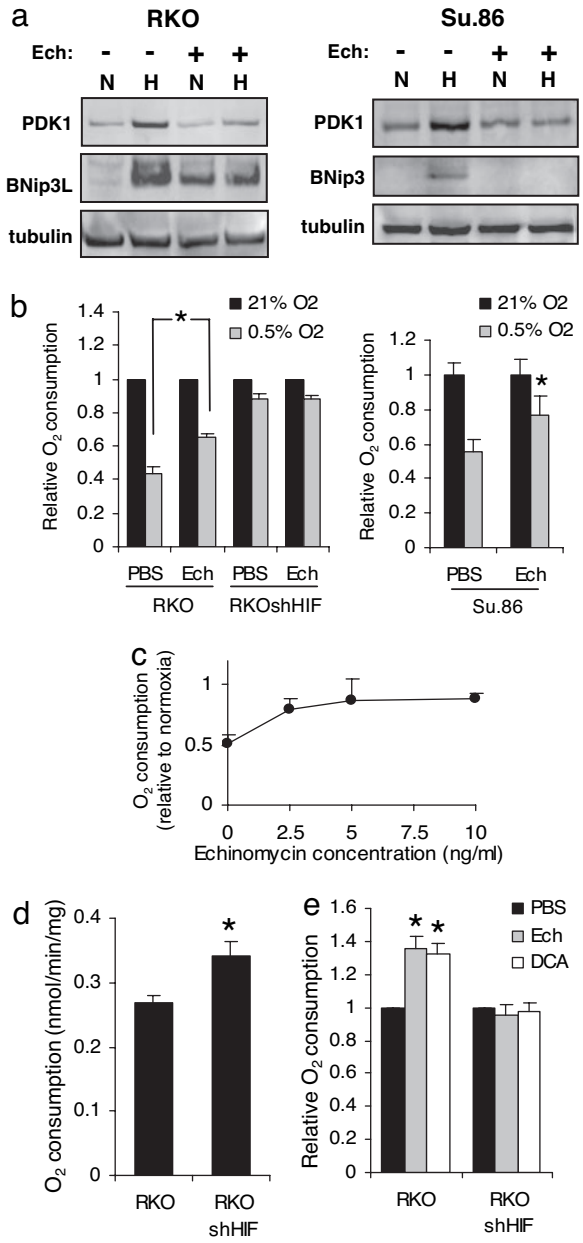

Fig. 1. Inhibition of HIF1 and PDK1 increases oxygen consumption *in vitro* and *in vivo*. (*a*) Western blots of extracts from RKO and Su.86 cells exposed to normoxia (N) or hypoxia (H) (0.5% O_2) for 24 h in the presence or absence of 2 ng/ml echinomycin probed for the indicated proteins. (*b*) Oxygen consumption rates of RKO and RKOShHIF1α cells (*Left*) and Su.86 cells (*Right*) after 24 h treatment with normoxia or hypoxia (0.5% O_2) with or without 2 ng/ml echinomycin. Data are normalized to normoxic samples. (*c*) Relative oxygen consumption of RKO cells treated with hypoxia (0.5% O_2) for 24 h in the presence of increasing concentrations of echinomycin. (*d*) Oxygen consumption rates of freshly explanted tumor tissue from RKO ($n = 16$) and RKOShHIF1α ($n = 8$) xenografts. (*e*) Oxygen consumption rates of RKO and RKOShHIF1α tumors from mice treated with 0.12 mg/kg echinomycin i.p. 24 h prior ($n = 8$), or 50 mg/kg DCA i.p. 4 h prior ($n = 8$). Data are normalized to PBS treated controls ($n = 8$–16). *, Significant difference relative to control ($P < 0.05$).

in immune-deficient mice, and oxygen consumption was measured in freshly explanted samples. Oxygen consumption per milligram of tumor was significantly higher in HIF1α knockdown samples than in WT RKO samples (Fig. 1*d*). These data are consistent with the existence of significant hypoxia in model tumors (24, 25), and the *in vitro* finding that hypoxia decreases oxygen consumption in a HIF-dependant manner. To examine the effect of acute HIF1 inhibition *in vivo*, tumor oxygen consumption was measured after animals were treated with echinomycin. Echinomycin significantly increased tumor oxygen consumption in RKO WT tumors but had no effect in RKOShHIF1α tumors, demonstrating that the pharmacologic target of echinomycin responsible for increasing oxygen consumption *in vivo* is HIF1 (Fig. 1*e*). To test whether this effect is mediated by the HIF1 target gene PDK1, we also measured oxygen consumption in tumors treated with the well-characterized PDK1 inhibitor DCA (21). Similar to the echinomycin treatment, DCA increased oxygen consumption in RKO tumors in a HIF1 dependent manner (Fig. 1*e*). Similar effects of both echinomycin and DCA were also observed in Su.86-derived tumors (SI Fig. 8).

Tissue oxygen concentration is determined by both oxygen supply and oxygen demand. Mathematical modeling of tumor oxygenation suggests that small changes in oxygen consumption can have a large impact on the extent of tumor hypoxia when compared with changes in oxygen delivery (26). We therefore established a reporter system that would allow us to monitor the biologic changes in tumor oxygen levels in response to the observed changes in oxygen consumption caused by HIF1 or PDK1 inhibition. RKO and RKOShHIF1α cells were stably transfected with a luciferase reporter gene under the control of a synthetic HIF1 responsive promoter consisting of 5 tandem repeats of a HIF binding site (5XHRE) (27). Luciferase activity in these cells provides a sensitive measure of hypoxia that can be monitored noninvasively over time both *in vitro* and *in vivo* by using bioluminescent imaging. When RKO reporter cells were exposed to hypoxia for 24 h *in vitro*, luciferase activity in WT cells increased $\approx$80 fold, whereas the increase in the RKOShHIF1α cells was $<$2 fold (Fig. 2*a*). The hypoxic induction of luciferase in RKO reporter cells *in vitro* was completely inhibited by echinomycin in a dose dependent manner (Fig. 2*b*).

We next tested the effect of DCA treatment on luciferase activity in RKO and RKOShHIF1α 5XHRE-luciferase reporter tumors to determine whether acutely increasing tumor oxygen consumption increases tumor hypoxia. Mice were implanted with one RKO and one RKOShHIF1α 5XHRE-luciferase reporter tumor on either flank, and luciferase activity was measured *in vivo*. After administration of DCA, the luciferase signal increased substantially in the WT, but not in the HIF1α knockdown tumors, supporting the hypothesis that increased oxygen consumption results in increased tumor hypoxia (Fig. 2 *c* and *d*). To establish that the *in vivo* luciferase signal reflects the hypoxic tumor cells, a group of RKO reporter tumors was imaged after a single dose of the hypoxic cytotoxin TPZ. TPZ has been shown to rapidly reduce the hypoxic fraction of experimental tumors by $>$10-fold (28). Twelve hours after TPZ treatment, the luciferase signal of HRE-reporter tumors was reduced by 90% (SI Fig. 9), showing that the luciferase signal emanating from the reporter tumors is coming primarily from the hypoxic, TPZ-sensitive cells.

Because echinomycin acts as a HIF inhibitor, the 5XHRE reporter system could not be used to monitor the effect of the drug on tumor hypoxia. As an alternative, the hypoxia marker drug pimonidazole was used to determine the hypoxic fraction of tumors treated with echinomycin. Mice bearing RKO and RKOShHIF1α tumors were treated with echinomycin or vehicle control, and pimonidazole was administered at 24 h to identify the hypoxic tumor cells. Fig. 3 shows sections from these tumors, stained with a FITC-conjugated monoclonal antibody against pimonidazole. The hypoxic fraction of each tumor was quantified by measuring the fraction of the viable tumor section that stained positive for pimonidazole. Echinomycin treatment caused an increase in the hypoxic fraction of RKO tumors, but

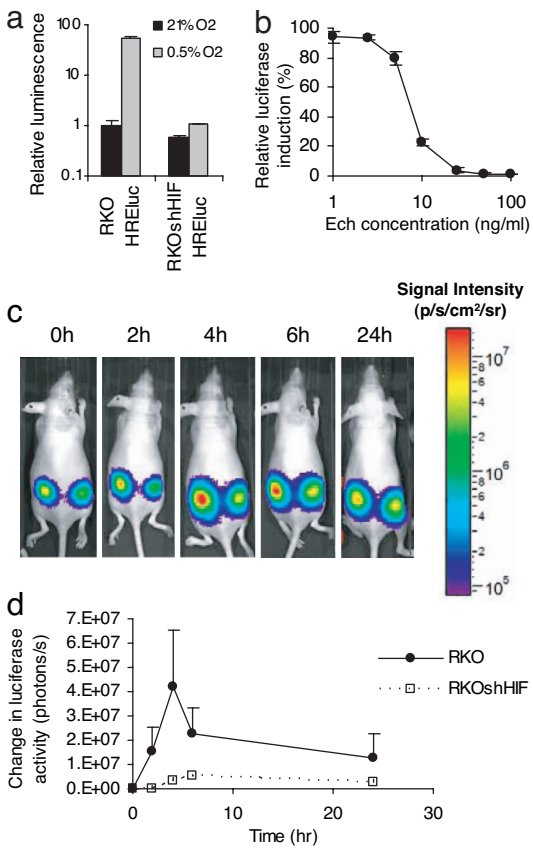

Fig. 2. Increasing oxygen consumption by inhibition of PDK activity increases tumor hypoxia. (*a*) Luciferase activity of WT and HIF1α knockdown RKO cells stably transfected with a HIF1 responsive luciferase reporter gene. Cells were exposed to 0.5% O_2 for 24 h in triplicate. Luminescence is normalized to normoxic HIF WT cells. (*b*) Luciferase activity of WT RKO HIF1 reporter cells exposed to 0.5% O_2 for 24 h in the presence of increasing concentrations of echinomycin. Data are normalized to the increase in signal observed in the absence of drug. (*c*) Bioluminescent imaging *in vivo*. Images show a representative animal bearing an RKO reporter tumor on the left flank and an RKOShHIF1α reporter tumor on the right flank as a function of time after i.p. injection of 50 mg/kg DCA. The pseudocolor overlay shows the intensity of bioluminescence. (*d*) Quantification of *in vivo* bioluminescence. The graph shows the change in signal intensity after DCA treatment for RKO parent and RKOShHIF1α tumors. The data represent the mean of three independent experiments, each comprising five RKO and five RKOShHIF1α reporter tumors.

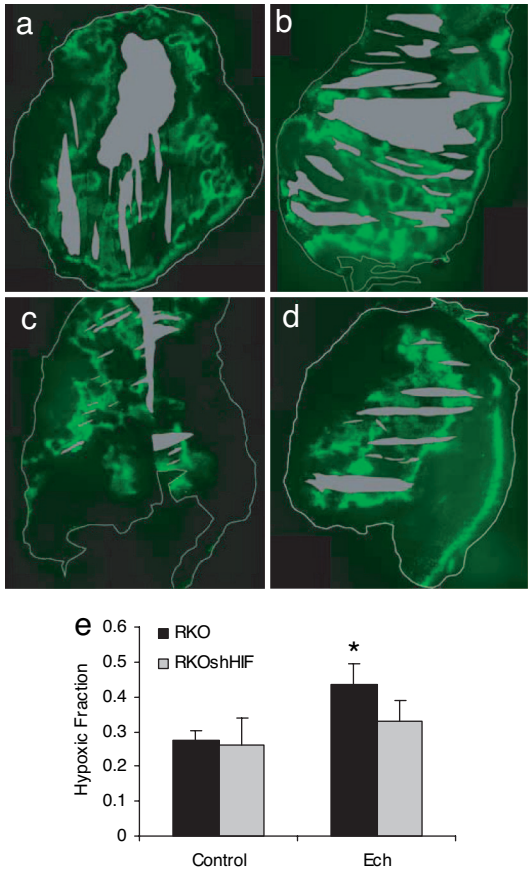

Fig. 3. Increasing oxygen consumption by inhibition of HIF increases tumor hypoxia. (*a–d*) Pimonidazole staining of tumor sections from RKO (*a* and *b*) and RKOShHIF1α (*c* and *d*) tumors 24 h after treatment with PBS (*a* and *c*) or echinomycin (*b* and *d*). The tumor section is outlined in white, pimonidazole staining is shown in green, and the necrotic areas and cutting artifacts are masked in gray. (*e*) The mean hypoxic fraction of RKO and RKOShHIF1α tumors 24 h after treatment with PBS or echinomycin (n = 4–5 tumors per group). Error bars represent the standard error of the mean. *, Significant difference ($P < 0.05$).

had no significant effect on the hypoxia in RKOShHIF1α tumors (Fig. 3*e*). There was no difference in other parameters such as the necrosis observed in the four treatment groups (data not shown).

Based on extensive experimental and clinical data, increasing the hypoxic fraction of solid tumors would be predicted to decrease the effectiveness of radiation therapy. However, hypoxic-specific cytotoxins such as TPZ show increased toxicity as oxygen concentration decreases (7, 29). Therefore, increasing the number of hypoxic tumor cells should enhance the efficacy of such drugs. To examine this possibility, we tested the ability of echinomycin and DCA to enhance the effectiveness of TPZ in a standard tumor growth delay assay. In both cases, treatment of RKO tumor bearing animals with the metabolic modifier before TPZ produced greater than additive tumor growth delay compared with single agents (Fig. 4 *a* and *b*). Treatment with echinomycin did not enhance the efficacy of etoposide, a drug whose toxicity is not dependant on oxygen concentration (Fig. 4*c*). If echinomycin acts as a metabolic modifier to enhance TPZ therapy, it should only be effective if given before the hypoxic cytotoxin. We tested this prediction by reversing the drug schedule, and found that treatment with TPZ followed by echinomycin had little effect on the growth of RKO, Su.86, or ras-transformed MEF tumors when compared with treatment with echinomycin followed by TPZ (Fig. 5 *a* and *c* and SI Fig. 10). To determine whether the molecular target of echinomycin *in vivo* responsible for its ability to sensitize tumors to TPZ was HIF1, we performed a similar growth delay experiment using RKOShHIF1α tumors. In this situation, echinomycin plus TPZ had no significant effect on tumor growth, regardless of the order that the drugs were given (Fig. 5*b*). These data provides genetic evidence that biochemical inhibition of HIF1 or its target gene PDK1 alters tumor metabolism, increases the degree of hypoxia, and sensitizes tumors to treatment with hypoxic cytotoxins such as TPZ.

Discussion

HIF1 has been shown to decrease mitochondrial oxygen consumption through the up-regulation of its target gene PDK1 (17), suggesting that inhibition of this pathway may represent a novel means of specifically altering the hypoxic microenvironment of solid tumors. The model predicts that inhibiting the transcriptional activity of HIF in solid tumors will block the

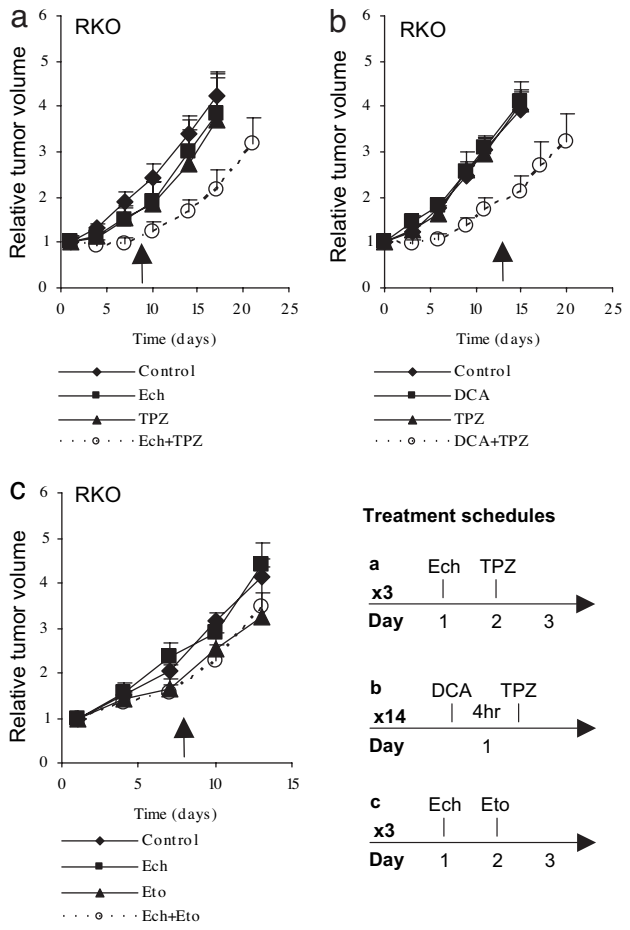

Fig. 4. Pharmacologic inhibition of HIF1 or PDK1 enhances the response of tumor xenografts to the hypoxic cytotoxin TPZ. (*a*) RKO tumor bearing mice were treated with 0.12 mg/kg echinomycin i.p. followed by 30 mg/kg TPZ i.p. at 24 h, followed by a rest day for 3 cycles. (*b*) RKO tumor-bearing mice were treated with 50 mg/kg DCA i.p. followed by 20 mg/kg TPZ i.p. at 4 h daily for 14 days. (*c*) RKO tumor-bearing mice were treated with 0.12 mg/kg echinomycin i.p. followed by 10 mg/kg etoposide i.p. at 24 h, followed by a rest day for 3 cycles. For all experiments, single agents were given at the same dose, on the same schedule. Arrows indicate the end of treatment.

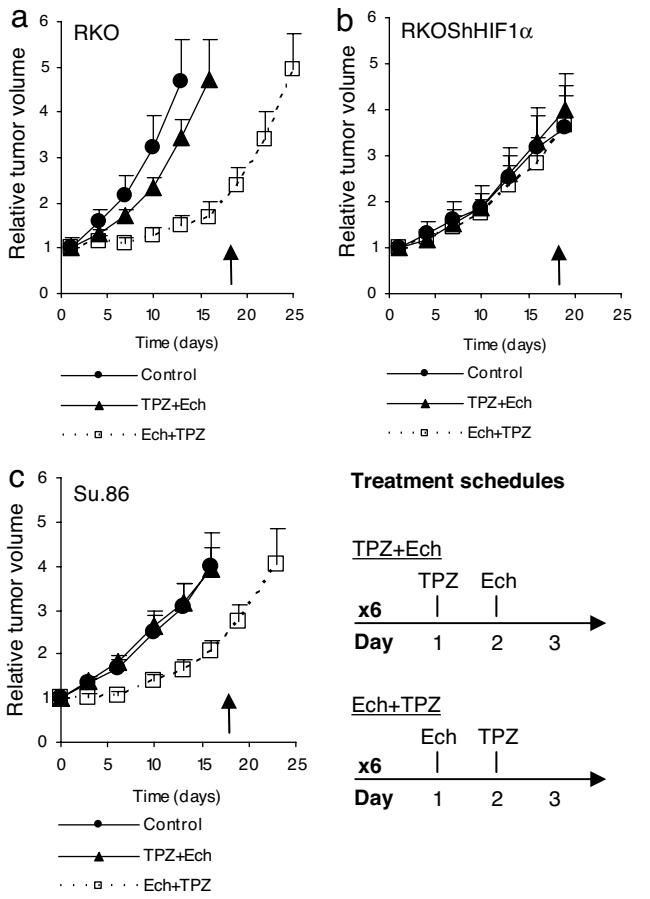

Fig. 5. Enhancement of TPZ efficacy is HIF-dependent and schedule-dependent. RKO (*a*), RKOShHIF1α (*b*), or Su.86 (*c*) tumor-bearing mice were treated with echinomycin followed by TPZ for six cycles (Ech+TPZ), or TPZ followed by echinomycin for 6 cycles (TPZ+Ech) as described above. Arrows indicate the end of treatment.

HIF-mediated adaptive response to hypoxia and result in an increase in the rate of oxygen consumption. This increased consumption of oxygen should lead to an increase in the extent of tumor hypoxia. Because hypoxia and HIF stabilization are situations encountered primarily in solid tumors, this strategy should not affect the metabolism of normal tissues.

Here, we show that biochemical inhibition of HIF or PDK1, by echinomycin or DCA respectively, increases the oxygen consumption rate of solid tumors. As predicted, this intervention results in an increase in tumor hypoxia as measured by using a bioluminescent hypoxia reporter system, or the hypoxia marker drug pimonidazole. These findings are consistent with models suggesting that tumor oxygenation is very sensitive to changes in oxygen consumption (26). Interestingly, although genetic inhibition of HIF1α in RKO cells resulted in increased tumor oxygen consumption, the hypoxic fraction and necrotic fraction of these tumors were not different from those of controls (Fig. 3). This finding suggests that during the course of tumor development, oxygen delivery may be increased in the HIF1α knockdown tumors, compensating for the increased oxygen demand.

Hypoxia decreases the effectiveness of radiation therapy and certain types of chemotherapy, and predicts for poor outcome in several human malignancies (1, 3–5, 8). Further, it has been shown to accelerate tumor progression and metastasis in experimental systems (30–33). Unfortunately, attempts to improve tumor oxygenation during therapy have not yielded clinically compelling results (1, 6). The alternative is to exploit the hypoxic microenvironment by designing therapies that take advantage of this unique property of solid tumors. Approaches currently under investigation include the use of anaerobic bacteria, hypoxia-specific gene therapy vectors, and bioreductive drugs that are converted to their cytotoxic forms under low oxygen conditions (7). Contrary to conventional treatments, it is predicted that these therapies should be more effective against more hypoxic tumors. In the case of TPZ, recent data support this concept, as the drug was found to have greater efficacy in treatment of more hypoxic tumor xenografts (34), and patients with more hypoxic tumors (35). We show here that decreasing tumor oxygenation by increasing oxygen consumption sensitizes tumors to treatment with TPZ. Although other groups have reported that HIF inhibitors may enhance the effectiveness of some chemotherapies (36) we observed no effect of echinomycin on the efficacy of etoposide, suggesting that this interaction is not a nonspecific sensitization. The lack of an effect in the RKO-ShHIF1α tumors demonstrates that the increased sensitivity is due to echinomycin's inhibition of HIF. Furthermore, the requirement that echinomycin be given before TPZ to achieve an effect shows that it is not acting by directly killing a complementary population of tumor cells, but rather by altering the

tumor microenvironment. This approach to the modification of tumor hypoxia should prove useful for other bioreductive drugs, and for other treatments that rely on the presence of hypoxia. This finding also suggests that targeting HIF before radiotherapy may lead to radiation resistance, because of an increase in hypoxic tumor cells. However, it has been shown that inducible siRNA against HIF can increase radiation effectiveness when HIF is inhibited after radiation, suggesting that HIF inhibition produces other effects that contribute to radiation sensitivity (37). More generally, these data emphasize that care should be taken in designing and scheduling therapeutic regimens that include agents capable of modifying the tumor microenvironment, to achieve maximal efficacy.

Currently, there is a great deal of interest in developing specific and potent HIF inhibitors for a variety of clinical applications (38). It has been suggested that HIF inhibitors may possess anti-tumor activity based on their effect on the tumor vasculature (39, 40). The results reported here provide a mechanism of action by which these inhibitors may be used therapeutically. Some tumors, like those derived from the RKO cell line, may be resistant to the anti-tumor activity of HIF1 blockade because of their genetic background or tumor type. However, these tumors may still be sensitive to the metabolic effects of HIF1 inhibition. As more of the downstream effects of HIF1 are elucidated, there may be more opportunities to sensitize tumors to cytotoxic therapies by manipulating tumor metabolism.

Materials and Methods

Cell Lines and Tumor Xenografts. RKO and Su.86 cells were obtained from the American Type Culture Collection (ATCC, Manassas, VA). HIF WT and knockout SV40-immortalized MEFs were a gift from R. Johnson (University of California, San Diego). MEFs were transformed by stable transfection with an activated H-ras expression plasmid. The RKOShHIF1α cell line has been described (17). RKO and MEF cells were grown in DMEM supplemented with 10% FBS. Su.86 cells were grown in RPMI medium 1640 supplemented with 10% FBS. Cells were exposed to hypoxia by placing culture dishes into an Invivo$_2$ humidified hypoxia workstation (Ruskin Technologies, Bridgend, U.K.) at 0.5% O_2. Echinomycin was a gift of A. Giaccia (Stanford University, Stanford, CA). TPZ was a gift of M. Brown (Stanford University, Stanford, CA). Etoposide (VP-16) was purchased from Sigma (St. Louis, MO). Tumor xenografts were established by injecting 5×10^6 RKO cells, 1×10^7 Su.86 cells, or 2×10^6 Hras-MEF cells s.c. into the flanks of 6- to 8-week-old female nude mice. Caliper measurements of two perpendicular diameters were used to monitor tumor growth (volume = $(d_1)(d_2)(d_2)(0.52)$). All animal protocols were approved by the Stanford Administrative Panel on Laboratory Animal Care.

Western Blots. Cells were harvested directly in RIPA buffer (0.15 mM NaCl/0.05 mM Tris· HCl, pH 7.2/1% Triton X-100/1% sodium deoxycholate/0.1% SDS) containing protease inhibitors. Protein concentrations were quantified (Pierce, Rockford, IL), and 25–50 μg of total protein was electrophoresed on a reducing Tris-Tricine gel and electroblotted to PVDF membrane. Antibodies used were rabbit anti-PDK1 (Stressgen, Victoria, Canada) (1:2,000), murine anti-α tubulin (Research Diagnostics, Concord, MA) (1:2,000), and rabbit anti-Bnip3 and anti-Bnip3L as described (41) (1:500). Primary antibodies were detected with species-specific secondary antibodies labeled with alkaline phosphatase (Vector Laboratories, Burlingame, CA) (1:3,000) and visualized with ECF (Amersham, Piscataway, NJ) on a Storm 860 PhosphorImager (Molecular Devices, Sunnyvale, CA).

Oxygen Consumption Measurements. Cells were trypsinized and suspended at 3×10^6 to 6×10^6 cells per ml in normoxic DMEM + 10% FBS. Oxygen consumption was measured in a 0.5-ml volume by using an Oxytherm electrode unit (Hansatech, Norfolk, U.K.) as described (17). To measure *in vivo* oxygen consumption, tumors were excised, and four samples per tumor, of ≈50 mg each, were weighed and thoroughly minced in DMEM + 10% FBS. Oxygen consumption was measured as above in a 1-ml volume and normalized to tissue weight.

Luciferase Reporter Assay. RKO and RKOshHIF1α cells were stably transfected with a luciferase reporter construct (5xHRE-luciferase) containing the firefly luciferase gene under the control of a synthetic HIF responsive promoter described (27). Cells were exposed to 0.5% O_2 for 24 h, and luciferase activity was measured in triplicate by using a luciferase reporter gene assay kit (Roche, Indianapolis, IN) and a Monolight 2010 luminometer (Analytical Luminescence Laboratory, San Diego, CA). For analysis of the effect of echinomycin on luciferase activity *in vitro*, 5×10^4 cells were seeded to 96-well plates, and, 24 h later, media were changed and drugs were added. Plates were placed in normoxic or hypoxic (0.5% O_2) incubators for 24 h and imaged directly in a Xenogen IVIS100 bioluminescent imaging system (Xenogen, Alameda, CA) in the presence of 150 μg/ml potassium *d*-luciferin (Xenogen).

Bioluminescent Imaging. Mice bearing 100–200 mm^3 s.c. HRE-luciferase reporter tumors were anesthetized by using 2% isofluorane and injected i.p. with 150 mg/kg potassium *d*-luciferin (Xenogen). After 10 min, bioluminescence was measured in a Xenogen IVIS100 system (Xenogen). Data were quantified by measuring total photons/s from uniform regions of interest. Data presented are the mean of three independent experiments, each comprising five RKO and five RKOShHIF1α tumors.

Detection of Tumor Hypoxia by Pimonidazole Immunofluorescence. Mice bearing 100–300 mm^3 RKO and RKOshHIF tumors on either flank were treated with 0.12 mg/kg echinomycin i.p. or saline control. After 24 h, they were injected with the hypoxia marker drug pimonidazole (60 mg/kg i.p.) (Millipore, Temecula, CA). Three hours later, tumors were excised and frozen in liquid nitrogen. Frozen sections (10 μm thick) from the central regions of tumors were fixed for 15 min in acetone at 4°C. Slides were blocked for 30 min in 4% FBS, 5% nonfat milk, and 0.1% Triton X-100 in PBS. Slides were incubated for 1 h at room temperature with an FITC-conjugated monoclonal antibody against pimonidazole (1:20) (Millipore) and counterstained with 50 nM propidium iodide (PI). FITC and PI fluorescent signals for entire tumor sections (one section per tumor) were acquired on a Nikon Eclipse E800 microscope equipped with a motorized scanning stage, a 12-bit QImaging camera (QImaging, Burnaby, Canada), and Bioquant imaging software (Bioquant, Nashville, TN). Acquisition parameters were constant for all samples. Tiled images were analyzed by using ImageJ software (NIH, Bethesda, MD). The area of the tumor section was manually defined by using the PI signal, and areas of necrosis and cutting artifacts were removed. The FITC-positive area was defined by using a common threshold value for all sections. The threshold value was chosen such that tumor sections from animals not injected with pimonidazole had no signal. The hypoxic fraction was defined as the FITC-positive area/the viable tumor area.

Tumor Growth Delay. When tumor volume reached 100–200 mm^3, mice were randomized to treatment groups. The echinomycin plus TPZ (or etoposide) groups were treated with 0.12 mg/kg echinomycin i.p. followed at 24 h by 30 mg/kg TPZ i.p. (or 10 mg/kg etoposide), followed by a rest day for three or six cycles. The DCA plus echinomycin treatment group was treated with 50 mg/kg DCA i.p. followed at 4 h by 20 mg/kg TPZ i.p. daily for 14 days. Single agents or saline controls were given at the same doses on the same schedules. For schedule dependence experiments, the doses were

the same as above, with the TPZ plus echinomycin group receiving TPZ, followed at 24 h by echinomycin, followed by a rest day for 6 cycles. Each treatment arm consisted of two independent groups of 6 to 8 tumors (12–16 total tumors per group).

Data Analysis. Changes in oxygen consumption, luciferase activity, hypoxic fraction, and tumor growth were analyzed by ANOVA, followed by pair-wise comparisons using a two-tailed Student's t test with the Bonferroni correction for multiple comparisons as needed. For all data, P values <0.05 were considered significant. All error bars represent the standard error of the mean.

This work was supported by funding from the National Cancer Institute (to N.C.D.). R.A.C. is a Research Fellow of The Terry Fox Foundation through an award from the National Cancer Institute of Canada.

1. Vaupel P (2004) *Semin Radiat Oncol* 14:198–206.
2. Brown JM, Giaccia AJ (1998) *Cancer Res* 58:1408–1416.
3. Brizel DM, Scully SP, Harrelson JM, Layfield LJ, Bean JM, Prosnitz LR, Dewhirst MW (1996) *Cancer Res* 56:941–943.
4. Fyles A, Milosevic M, Hedley D, Pintilie M, Levin W, Manchul L, Hill RP (2002) *J Clin Oncol* 20:680–687.
5. Nordsmark M, Overgaard J (2004) *Acta Oncol* 43:396–403.
6. Kaanders JH, Bussink J, van der Kogel AJ (2004) *Semin Radiat Oncol* 14:233–240.
7. Brown JM, Wilson WR (2004) *Nat Rev* 4:437–447.
8. Cairns R, Papandreou I, Denko N (2006) *Mol Cancer Res* 4:61–70.
9. Li F, Wang Y, Zeller KI, Potter JJ, Wonsey DR, O'Donnell KA, Kim JW, Yustein JT, Lee LA, Dang CV (2005) *Mol Cell Biol* 25:6225–6234.
10. Elstrom RL, Bauer DE, Buzzai M, Karnauskas R, Harris MH, Plas DR, Zhuang H, Cinalli RM, Alavi A, Rudin CM, Thompson CB (2004) *Cancer Res* 64:3892–3899.
11. Matoba S, Kang JG, Patino WD, Wragg A, Boehm M, Gavrilova O, Hurley PJ, Bunz F, Hwang PM (2006) *Science* 312:1650–1653.
12. Denko NC, Fontana LA, Hudson KM, Sutphin PD, Raychaudhuri S, Altman R, Giaccia AJ (2003) *Oncogene* 22:5907–5914.
13. Fantin VR, St-Pierre J, Leder P (2006) *Cancer Cell* 9:425–434.
14. Seagroves TN, Ryan HE, Lu H, Wouters BG, Knapp M, Thibault P, Laderoute K, Johnson RS (2001) *Mol Cell Biol* 21:3436–3444.
15. Semenza GL, Artemov D, Bedi A, Bhujwalla Z, Chiles K, Feldser D, Laughner E, Ravi R, Simons J, Taghavi P, Zhong H (2001) *Novartis Found Symp* 240:251–260.
16. Semenza GL (2003) *Nat Rev* 3:721–732.
17. Papandreou I, Cairns RA, Fontana L, Lim AL, Denko NC (2006) *Cell Metab* 3:187–197.
18. Kim JW, Tchernyshyov I, Semenza GL, Dang CV (2006) *Cell Metab* 3:177–185.
19. Hagen T, Taylor CT, Lam F, Moncada S (2003) *Science* 302:1975–1978.
20. Kong D, Park EJ, Stephen AG, Calvani M, Cardellina JH, Monks A, Fisher RJ, Shoemaker RH, Melillo G (2005) *Cancer Res* 65:9047–9055.
21. Stacpoole PW, Nagaraja NV, Hutson AD (2003) *J Clin Pharmacol* 43:683–691.
22. Dang DT, Chen F, Gardner LB, Cummins JM, Rago C, Bunz F, Kantsevoy SV, Dang LH (2006) *Cancer Res* 66:1684–1693.
23. Mizukami Y, Jo WS, Duerr EM, Gala M, Li J, Zhang X, Zimmer MA, Iliopoulos O, Zukerberg LR, Kohgo Y, *et al*. (2005) *Nat Med* 11:992–997.
24. Adam MF, Dorie MJ, Brown JM (1999) *Int J Radiat Oncol Biol Phys* 45:171–180.
25. Rockwell S, Moulder JE (1990) *Int J Radiat Oncol Biol Phys* 19:197–202.
26. Secomb TW, Hsu R, Ong ET, Gross JF, Dewhirst MW (1995) *Acta Oncol* 34:313–316.
27. Shibata T, Giaccia AJ, Brown JM (2000) *Gene Ther* 7:493–498.
28. Kim IH, Brown JM (1994) *Int J Radiat Oncol Biol Phys* 29:493–497.
29. Koch CJ (1993) *Cancer Res* 53:3992–3997.
30. Subarsky P, Hill RP (2003) *Clin Exp Metastasis* 20:237–250.
31. Cairns RA, Hill RP (2004) *Cancer Res* 64:2054–2061.
32. Bedogni B, Welford SM, Cassarino DS, Nickoloff BJ, Giaccia AJ, Powell MB (2005) *Cancer Cell* 8:443–454.
33. Erler JT, Bennewith KL, Nicolau M, Dornhofer N, Kong C, Le QT, Chi JT, Jeffrey SS, Giaccia AJ (2006) *Nature* 440:1222–1226.
34. Emmenegger U, Morton GC, Francia G, Shaked Y, Franco M, Weinerman A, Man S, Kerbel RS (2006) *Cancer Res* 66:1664–1674.
35. Rischin D, Hicks RJ, Fisher R, Binns D, Corry J, Porceddu S, Peters LJ (2006) *J Clin Oncol* 24:2098–2104.
36. Li L, Lin X, Shoemaker AR, Albert DH, Fesik SW, Shen Y (2006) *Clin Cancer Res* 12:4747–4754.
37. Moeller BJ, Dreher MR, Rabbani ZN, Schroeder T, Cao Y, Li CY, Dewhirst MW (2005) *Cancer Cell* 8:99–110.
38. Melillo G (2006) *Mol Cancer Res* 4:601–605.
39. Hickey MM, Simon MC (2006) *Curr Top Dev Biol* 76:217–257.
40. Kung AL, Zabludoff SD, France DS, Freedman SJ, Tanner EA, Vieira A, Cornell-Kennon S, Lee J, Wang B, Wang J, *et al*. (2004) *Cancer Cell* 6:33–43.
41. Papandreou I, Krishna C, Kaper F, Cai D, Giaccia AJ, Denko NC (2005) *Cancer Res* 65:3171–3178.